J. Fluid Mech. (1985), *vol.* 158, *pp.* 113–135
Printed in Great Britain

Characteristics of pressure-wave propagation in a compliant tube with a fully collapsed segment

By MASASHI SHIMIZU

Department of Control Engineering, Tokyo Institute of Technology,
Oh-Okayama, Meguro-ku, Tokyo

(Received 20 August 1984 and in revised form 7 March 1985)

In order to model the fluid dynamics of Korotkoff sound generation when the artery under the cuff is fully collapsed during most of the heart cycle, the characteristics of pressure-wave propagation in a long silicone-rubber tube were studied experimentally. The central portion of this tube was designed to collapse to zero cross-sectional area as a result of high negative transmural pressure, thus simulating a collapsed artery. Propagation of a single half-sinusoidal pressure wave in and around this segment was studied in detail by pressure, velocity and tube-longitudinal-shape measurements.

A very steep wave front (shock wave) capable of producing a short tapping sound was formed by an overtaking phenomenon in the fully collapsed tube segment and it propagated into the inflated tube distal to the collapsed segment. An empirical equation relating the flow rate penetrating into the collapsed segment, the incident-wave pressure and the external pressure P_c over the collapsed segment was obtained. This equation predicts that the pressure-wave propagation in a fully collapsed segment depends only on the flow rate into the collapsed segment.

The initial internal pressure of the tube distal to the collapsed segment P_{dd} is one independent variable in the high-cuff-pressure condition. The amplitude of the steep wave front and the shape of the pressure wave in the inflated tube distal to the collapsed segment are governed by $P_c - P_{dd}$ and the flow rate penetrating the collapsed segment. For the same flow rate, if $P_c - P_{dd}$ is lower than a critical value, the amplitude of the pressure in the distal tube decreases with increasing P_{dd} because of positive pressure-wave reflection at the exit of the collapsed segment. On the other had, if $P_c - P_{dd}$ is higher than that value, no wave reflection occurs and the amplitude of the pressure wave is independent of P_{dd}. In the latter case a severe constriction exists near the distal end of the collapsed segment, and flow occurs as two thin high-speed jets.

1. Introduction

In the auscultatory technique, the most widely used clinical method of non-invasive blood-pressure measurement, the systolic and the diastolic arterial blood pressures are taken as the pressure of the pneumatic cuff when the first and the last Korotkoff sound respectively are monitored. This technique was proposed by Korotkoff in 1905 with a simple qualitative explanation of the mechanism of sound generation. Since then many studies have been conducted, and the technique has been accepted and become the most popular one. However, the actual mechanism of sound generation has become a matter of dispute, and only recently has a satisfactory explanation been developed (McCutcheon & Rushmer 1967; Pedley 1980; Shimizu & Tanida 1983).

In a recent paper (Shimizu & Tanida 1983) the origin of Korotkoff sound was studied analytically and experimentally for diastolic-pressure measurement. In this case the cuff pressure is a little higher than the diastolic arterial pressure, and hence the artery under the cuff is partially collapsed when the arterial pulse from the heart arrives at the proximal end of the collapsed arterial segment. It was shown that Korotkoff sound is produced by the steep pressure-wave front (shock wave) formed during pressure-wave propagation in the partially collapsed vessel segment. The mechanism of sound generation for higher cuff pressure, however, remained unknown.

When audible Korotkoff sound is emitted from the artery distal to the cuff, an arterial pressure pulse with steep wave front is always detected, and the sound synchronizes with the steep wave front (Wallace, Lewis & Khlil 1961; London & London 1964, 1967; Burch & De Pasquale 1962). Thus the sound generation mechanism for higher cuff pressures should also be obtainable provided the fluid dynamics of the steep pressure-wave front is understood. When the artery under the cuff completely collapses over most of the arterial pulse cycle, some hypotheses, such as 'self-excited oscillation' (Ur & Gordon 1970; Lighthill 1972; Pedley 1980), are also available. The present author, however, feels that this case should be treated as one of nonlinear propagation of the arterial-pressure waves in the fully collapsed vessel segment.

To date, the propagation of finite-amplitude pressure waves in a fully collapsed compliant vessel has not been studied, and hence its characteristics are unknown. If pressure-wave propagation in a severely collapsed vessel is treated as an inviscid one-dimensional flow, the flow is readily predicted to become supercritical, and, as a result, the fluid flows through narrow channels at very high speed. Thus, in analysing real situations, fluid viscosity must be considered. However, it is not easy to treat such a viscous unsteady flow analytically. Furthermore, in some high-cuff-pressure cases, wave propagation at the downstream junction of the fully collapsed and inflated tube segments cannot be treated analytically using a simple one-dimensional-flow model and a ring-tube model. So, in this paper, the phenomenon is studied in detail experimentally. To treat pressure-wave propagation in a fully collapsed vessel segment, a simplified model similar to that used in the previous study (Shimizu & Tanida 1983) was selected instead of one attempting to simulate the real arterial system.

2. Experimental apparatus and procedure

The experimental apparatus is shown in figure 1. It consists of a pump (a), silicone-rubber tubes of 10 mm outer diameter and 0.4 mm wall thickness (b), a pressure box (c), two water reservoirs (d, e), a syringe (f) and a microphone with plastic sleeve (g). The pump, simulating the heart, is the same as that used in the previous experiment (Shimizu & Tanida 1983) and generates a single half-sinusoidal pressure wave, whose amplitude and period can be arbitrarily varied within the available range.

A silicone-rubber tube was selected as the model artery because of its transparency, which makes fluid-velocity measurement in the tube possible using a laser-Doppler velocimeter (LDV). The tube is divided into three segments, one in the box and the other two out of the box. The length of the segments proximal and distal to the box are 2.2 and 10 m respectively. The distal segment is long enough to eliminate completely the effect of the reflection wave, but the proximal segment is not. Therefore the reflected wave from the collapsed segment is rereflected at the pump

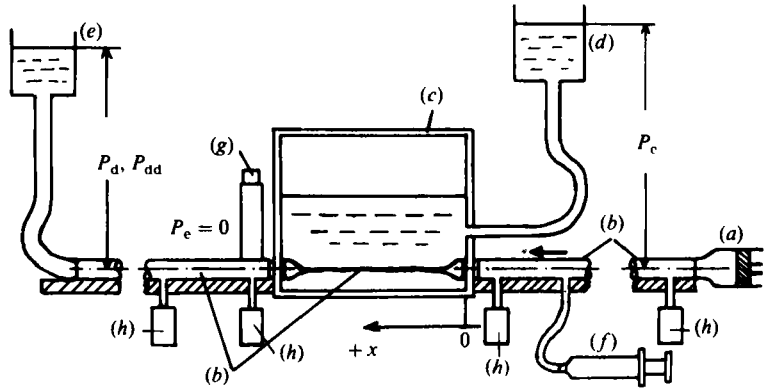

FIGURE 1. Schematic diagram of experimental apparatus: (*a*) mechanical pump; (*b*) silicone-rubber tube; (*c*) pressure box; (*d*) water reservoir for box pressure, P_c setting; (*e*) water reservoir for initial tube pressure, P_d or P_{dd} setting; (*f*) syringe for P_d setting; (*g*) microphone; (*h*) electrical pressure transducer; x, axial length coordinate to indicate location of measurement.

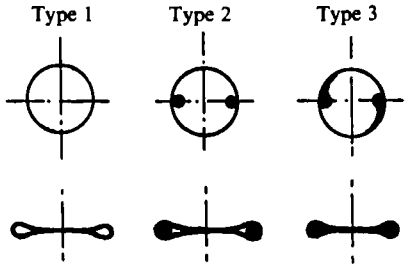

FIGURE 2. Schematic diagrams of cross-sections of three tube types in inflated and fully collapsed conditions.

and follows behind the incident pressure wave. (However, this was checked and found not to affect wave propagation.) On the bottom of the tubes, several pressure taps for measurement of the tube internal pressure P are set. The three tube segments are connected by two brass tubes of 10 mm outer diameter, 0.4 mm wall thickness and 3 cm length, which penetrate the two sidewalls of the pressure box. It was confirmed analytically and experimentally that the effect of the brass-tube insertion on wave propagation in inflated tubes is negligibly small for pressure waves of frequency lower than 10 Hz. The higher-frequency components of the pressure wave may be affected, but the overall effect on pressure-wave propagation is not considered to be large. In the collapsed-tube condition the effect is difficult to estimate, but there was little difference between the experimental results for 10 and 30 mm long brass tubes.

For the tube segment in the box, three types of tube shown in figure 2 are used. Type 1 is an intact tube. Types 2 and 3 were processed so that their tube laws (the relationship between tube cross-sectional area A and the transmural pressure across the tube wall) are similar to those of an artery. That is, A becomes almost zero when the tube collapses fully. For type 2 two silicon-rubber tubes of 2 mm diameter and 17 cm length, with both ends closed, were inserted and glued at the four locations along the axis, as seen in figure 2. Therefore the cross-sectional area in the fully collapsed condition is smaller than that of type 1, but not zero. In type 3 silicone rubber for casting was poured into the cavity of the rubber tube, which was compressed at a transmural pressure of about -2.5 kPa, and hardened. Therefore

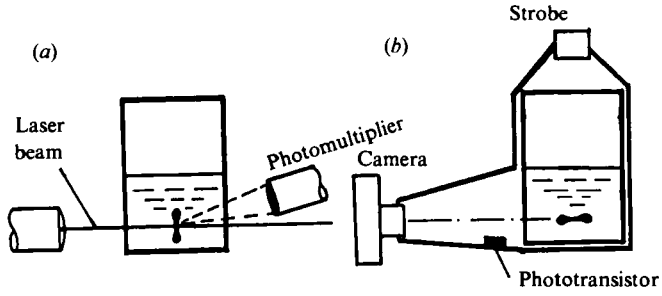

FIGURE 3. Schematic diagrams of equipments setting: (*a*) velocity measurement with laser-Doppler velocimeter; (*b*) taking pictures of the longitudinal shape of the collapsed tube segment.

type 3 has almost zero cross-sectional area for transmural pressures lower than -2.5 kPa. In all cases, the tube in the box is stretched longitudinally about 2.5 %. The length of the rubber tube between the two brass tubes is 17.4 cm.

The pressure box ((*c*) in figure 1), simulating a pneumatic cuff, is made of transparent plastic plates and filled with water up to half its height. The depth of the water is about 5 cm and the distance between the free surface of the water and the rubber tube axis is about 3 cm. The pressure in the box, P_c (which corresponds to the cuff pressure), is set arbitrarily by changing the height of the water reservoir (*d*).

The experimental procedure is as follows. First the initial tube internal pressure P_d and the box pressure P_c are set. All the pressures are measured relative to the atmospheric pressure. The initial condition simulates the diastolic state of the brachial artery when the auscultatory method is applied; therefore P_d corresponds to the diastolic blood pressure. In most experiments, the P_d values in the proximal and distal tubes are the same and can be set arbitrarily by changing the height of the water reservoir (*e*). However, in experiments in which the tube in the box is fully collapsed, they may be different. In this case, the initial tube internal pressure of the proximal tube is referred to as P_d and that of the distal tube as P_{dd}. P_d in this case is set with the aid of the syringe (*f*). In all cases, P_d and P_{dd} are set high enough to inflate the tubes outside of the box.

After setting P_d, P_{dd} and P_c, a half sinusoidal pressure wave is produced by the pump and its propagation studied. In the inflated tubes proximal and distal to the box, pressure and velocity are measured by the pressure transducers and the one-dimensional forward-scatter LDV system. For the collapsed tube segment in the box, pressure-wave propagation is studied by fluid-velocity measurement with LDV and by photographically recording the longitudinal shape of the tube (figure 3). During velocity measurement, the tube is set so that it collapses vertically. However, in taking pictures of the tube shape, the tube is rotated so as to collapse horizontally and the entire pressure box is put in a dark room, in which a strobe and a camera are set. The timing of strobe flashing is set arbitrarily by using a delay circuit triggered by pump action and monitored by a phototransistor and marked on the record of the pressure waveform taken at the same time. Changing the timing and repeating the same experiments, a series of still photographs which show time-serial change of the tube longitudinal shape are taken.

The location of pressure or flow-velocity measurement is expressed by the length x, which is measured from the inside surface of the box's proximal wall and takes positive values in the distal region and negative values in the proximal. The origin of the unsupported collapsible tube (in the box) is $x = 0.9$ cm.

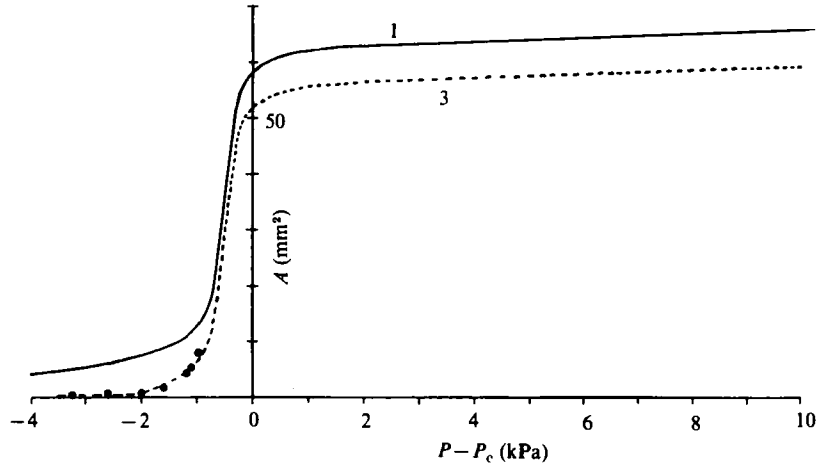

FIGURE 4. Tube laws of types 1 and 3 tubes.

3. Experimental results and discussion

3.1. *The effect of the tube law in the fully collapsed condition*

The most characteristic distinction between the tube laws of arteries and rubber tubes occurs in the fully collapsed condition. The internal cross-sectional area of an artery in this condition is assumed to be zero, while that of a rubber tube is typically small but not zero. Many kinds of rubber tubes are commonly used as model arteries. However, to date the effect of the difference in tube laws in the fully collapsed condition on pressure-wave propagation and Korotkoff sound generation has not been studied. Therefore it is studied using the three types of tube mentioned above.

The static tube laws of type 1 and 3 tubes are shown in figure 4. The solid line is for type 1 tubes, as measured when the transmural pressure $P-P_e$ is increasing using a 1 m long tube. The broken line is the tube law predicted for type 3 by subtracting the cross-sectional area of the cast silicon rubber from the cross-section of the type 1 tube. The dark circles indicate the type 3 tube law measured during a steady-flow experiment. In this case the flow rate Q through the collapsed tube segment is measured in a very small pressure gradient condition (0.05 kPa/16 cm) and A is then calculated from Q and the pressure difference by assuming the flow to be Poiseuille in the two circular tubes. Type 3 tubes have an almost zero cross-sectional area for $P-P_e < -2$ kPa. The tube law for type 2 has not been measured, but is assumed to lie between those of types 1 and 3.

In figure 5 the pressure-wave forms measured at the box exit ($x = 21.5$ cm) are shown for various box pressures. The change in the pressure-wave form due to P_e change will be discussed in detail later. However, for the moment we are only concerned with the effects of the tube type.

When P_e is low and the tube segment in the box is inflated or partially collapsed, no significant variation is observed in the pressure waves in the three tube types. The pressure wave at $x = 21.5$ for $P_e = 0$ is shown in figure 5(*a*) by a dotted broken line.

When P_e is increased and the segment in the box collapses fully, a consistent difference with tube type appears in the front portion FP of the pressure wave at the box exit. However, the main portion of the pressure wave MP following FP is not as strongly affected by tube type. Since in type 3 tube A in the fully collapsed condition is almost zero, a pressure wave travelling through the collapsed segment,

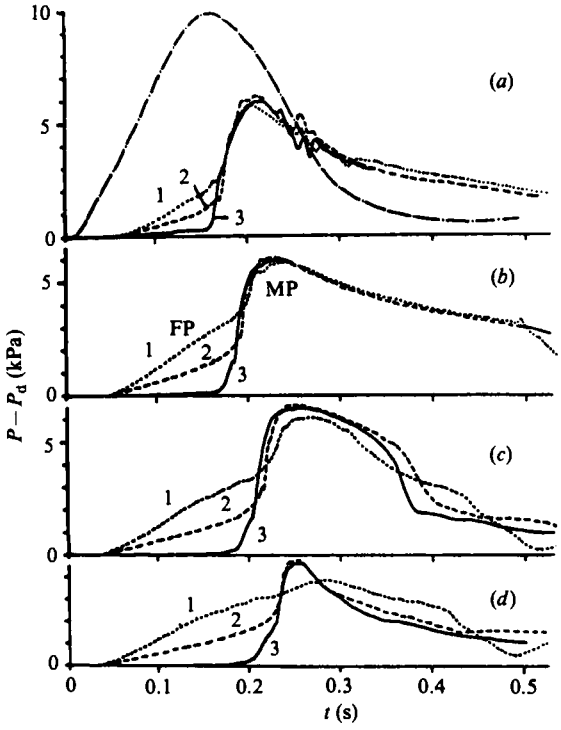

FIGURE 5. Comparison of pressure waveforms for the three tube types measured just distal to the box ($x = 21.5$ cm); for all figures $P_d = 4$ kPa, and 1, 2 and 3 represent types 1, 2 and 3 respectively: (*a*) dash–dot curve, $P_d - P_c = 4$ kPa, for other curves $P_d - P_c = -2$ kPa; (*b*) $P_d - P_c = -4$; (*c*) $P_d - P_c = -6$; (*d*) $P_d - P_c = -8$ kPa.

and producing the MP on its arrival at the box exit, may be assumed to force the tube into a partially collapsed condition. Therefore the FP is assumed to be produced by flow through narrow channels in the fully collapsed tube segment which exists between the box exit and the front of the main pressure wave travelling distally in the box, and hence decreases in length with time. The pressure at the moving proximal end of the collapsed segment is nearly equal to P_c, because the tube is in a partially collapsed condition. However, the pressure at its distal end, the box exit, increases with flow-rate increment. Therefore the incremental rate of pressure at the box exit due to this flow is expected to be gradual, and this expectation agrees well with the experimental results shown in figure 5. This flow is not expected to produce a phenomenon generating sharp Korotkoff sound.

On the other hand, as seen in figure 5, the gradient at the front of the MP is very steep in all tube types, and, as shown later, a sharp sound is generated, which synchronizes with the steep wave front. Therefore it is felt that the main portion of the wave is the most important when Korotkoff sound generation is considered.

From these experimental results and considerations, it can be concluded that whether a tube in fully collapsed condition has zero cross-sectional area or not is not essential in Korotkoff sound generation at high box pressures. The amplitude of the steep wave front of the main portion, however, is highest for type 3 tubes, for which the tube law most closely resembles that of an artery. Therefore we will be concerned primarily with type 3 tubes below. However, type 2 tubes are needed in some velocity and axial tube-shape measurements, because the cast silicone rubber

in the type 3 tube is opaque, and hence fluid-velocity measurement at locations other than the centre is impossible.

3.2. *Pressure-wave propagation for inflated or partially collapsed cases*

Inflated-tube case; $P_c = 0$

The pressure-wave propagation characteristics for the fully inflated condition of the tube segment in the box, $P_c = 0$, are the basis for study of the effect of tube collapse and hence will be examined first. From the relation between the measured pressure P and the central axial velocity U, the propagation of the pressure wave used in this experiment is known to be approximately linear for the inflated-tube condition. Thus in simple wave propagation without steady flow, the P versus mean velocity U_m relation is expressed as follows (Kamm & Shapiro 1979):

$$U_m = \frac{P - P_d}{\rho C}, \tag{1}$$

where P_d is the initial tube internal pressure, C is the pressure-wave propagation velocity and ρ is the density of the water. The experimentally obtained value of C from the P versus U relation and the propagation of peak pressure is 13 m/s.

Partially collapsed case

The characteristics of pressure-wave propagation through the partially collapsed tube segment in the box have already been reported (Shimizu & Tanida 1983). However, the rubber tube used in this study is different from the one used before, and so it is examined again for confirmation.

The pressure waveforms for various P_c values, measured at locations just proximal and distal to the pressure box ($x = -2.5$ and 21.5 cm respectively), are shown in figure 6 (a, b). The characteristics of pressure-wave deformation are as reported before, except for some minor changes. When collapse of the tube in the box is modest (A, B, C and D) the pressure waves at the box exit ($x = 21.5$ cm, figure 6b) consist of a steep wave front (shock wave SW) and a smooth portion roughly similar to that in the fully inflated condition (A). The steep wave front is preceded by a stronger negative wave than in the earlier experiment (Shimizu & Tanida 1983). The negative wave is found to become stronger with increase in the axial tension, and hence is considered to be the same as the wave induced by axial tensions reported by Kececioglu *et al.* (1981) and Jan, Kamm & Shapiro (1983). In the former experiment, the axial tension was zero and lower than that in the present study. At the proximal side to the box ($x = -2.5$ cm, figure 6a), the amplitudes of the pressure waves are lower than those of the incident waves (A) (because of negative wave reflection) until the arrival of the reflected shock wave (RSW) from the distal end of the collapsed-tube segment. The reflected shock in this study is much steeper than that in the earlier study. After the arrival of RSW, the pressure-wave forms become identical with those of the incident waves.

When the pressure P_c in the box is increased and the initial tube collapse becomes severe (E and F), the pressure waveform at $x = 21.5$ changes, and the steepness and amplitude of the wave front and the amplitude of the negative spike in front of it decrease with increase in P_c. However, after arrival of the rereflected shock wave (RRSW) from the proximal end of the collapsed segment, the pressure waves again become identical with those of the fully inflated case (A) for a short while. In the former study, RRSW were not observed. This is considered to be due to differences

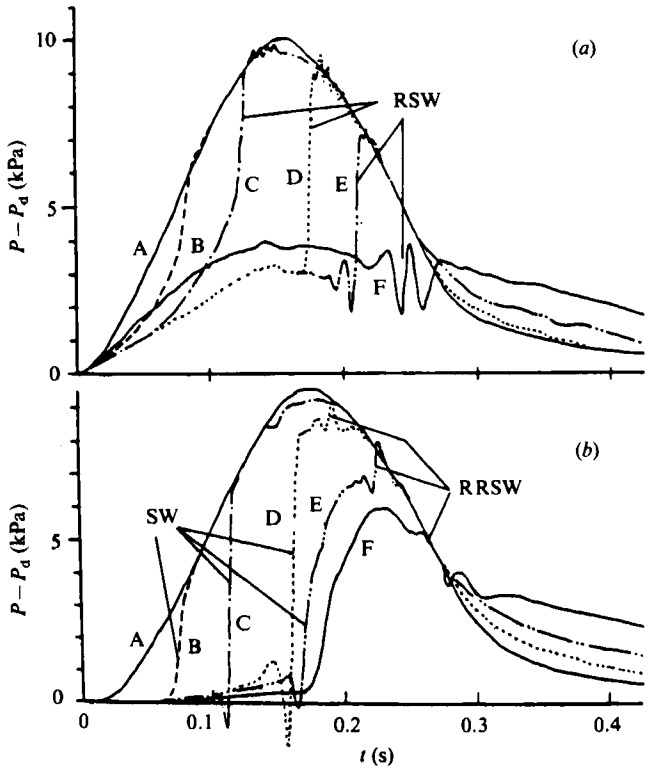

FIGURE 6. Pressure waves for inflated and partially collapsed conditions of the tube segment in the box, $P_d = 4$ kPa: (*a*) at $x = -2.5$ cm, RSW, reflected shock wave; (*b*) at $x = 21.5$ cm, SW, shock wave; RRSW, rereflected shock wave; A, $P_d - P_c = 4$ kPa; B, -0.2 kPa; C, -0.44 kPa; D -0.7 kPa; E, -1.0 kPa; F, -2.0 kPa.

in the stroke of the piston pump. That is, the present stroke is twice the former one and the rotation speed of the pump is about half the former value.

3.3. *Fully collapsed case* ($P_d - P_c < -3.0$ *kPa*)

The pressure waveforms, measured at the inlet ($x = -2.5$) and the exit of the box ($x = 21.5$), for various P_c values in the fully collapsed condition of the tube are shown in figure 7. As seen in figure 7i(*a*) and ii(*a*), at the box inlet the dependence of the pressure waveform change on the box pressure is systematic. However, it is complicated at the box exit, as seen in the figure 7i(*b*) and ii(*b*). This suggests that the phenomenon occurring at the inlet is simple, but at the exit is more complicated. Therefore they are treated separately in the following.

3.3.1. *Reflection and penetration of pressure wave at the box inlet*

Here, the waveforms shown in figure 7i(*a*) and ii(*a*) are considered. Even when the tube in the box is initially fully collapsed, a reflected shock RSW from the collapsed-segment distal end is seen in low-P_c cases. Excepting RSW, however, the pressure waves at $x = -2.5$ cm are deformed in a similar way in all P_c cases. Specifically, the pressure waves consist of a rapidly increasing front portion (FP), an almost-constant central portion (CP) and a rapidly decreasing tail portion (TP). The transition from FP to CP is gradual, but from CP to TP it is more sharp and occurs

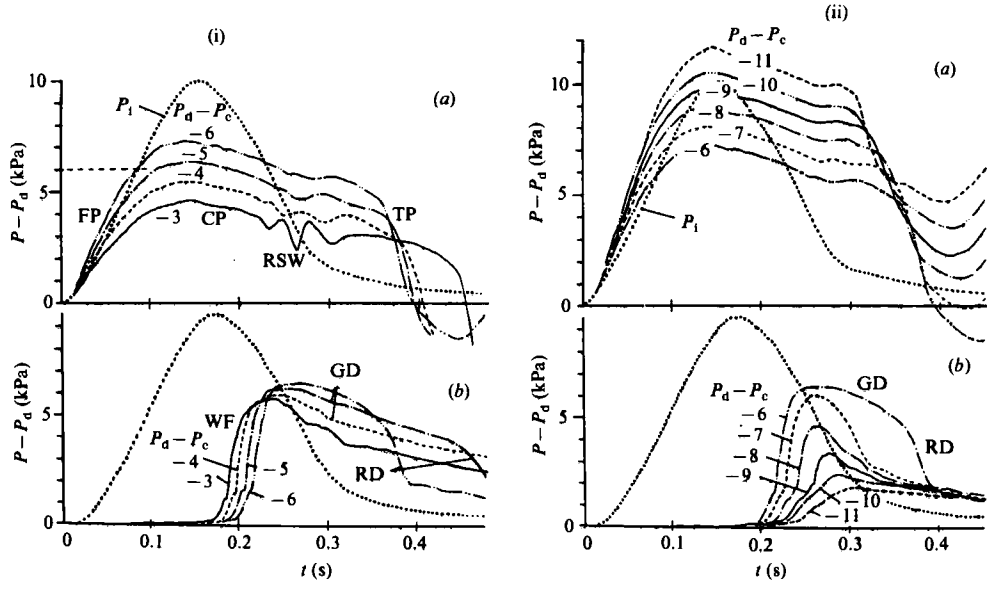

FIGURE 7. Pressure waves for various P_c-P_d values in the fully collapsed condition of the tube segment in the box: (i) for $P_d-P_c=-3$ to -6; (ii) for $P_d-P_c=-6$ to -11, $P_d=4$ kPa: (*a*) measured at $x=-2.5$ cm; P_i, incident pressure wave; FP, front portion; CP, central portion of almost constant pressure; TP, tail portion of rapid pressure decrement; (*b*) measured at $x=21.5$ cm; WF, Wave front; GD, gradual-decrement portion; RD, rapid-decrement portion.

always at $P\approx P_c-1.4$ kPa. The mean pressure of CP portion is higher than P_c by about 1 kPa for all P_c values.

The pressure-wave deformation mentioned above is caused by wave reflection from the fully collapsed segment in the box, whose impedance is very different from that of the inflated segment. Kenner (1976) has discussed a similar wave reflection. In order to explain the deformation of the pressure wave and to estimate the effect of P_c on the flow rate penetrating into the collapsed segment, an idealized tube model is now introduced. As shown in figure 4, the special feature of the tube law of the tube segment in the box is that A is almost zero for P lower than a critical pressure $P_c-\Delta P$, and the compliance becomes very high for $P>P_C-\Delta P$. To incorporate this characteristic, the tube law of the idealized model is assumed to be $A=0$ for $P<P_c-\Delta P$ and $\mathrm{d}A/\mathrm{d}P=\infty$ for $P>P_c-\Delta P$. Now let us consider what happens when the incident pressure wave $P_i(t)$ reaches the inlet of the idealized model tube ($X=0$). Initially $P_d<P_c-\Delta P$, and hence A for the tube in the box is zero. This is equivalent to the tube proximal to the box having a closed end. Therefore when the amplitude of the incident pressure wave $P_i(t)-P_d$ is low it is reflected completely at $x=0$. Thus

$$U=0,\quad P=2(P_i(t)-P_d)+P_d \quad \text{for } P_i(t)-P_d<\tfrac{1}{2}(P_c-\Delta P-P_d). \tag{2}$$

When $P_i(t)-P_d$ increases with time and $2(P_i(t)-P_d)+P_d$ becomes greater than $P_c-\Delta P$ the tube in the box starts to open. In this situation $\mathrm{d}A/\mathrm{d}P$ for the tube becomes ∞, and hence the static pressure in the tube in the box becomes constant at $P_c-\Delta P$. To determine the pressure proximal to the box, the flow rate and A for the collapsed segment must be known. However, from the results of the flow-velocity measurement (considered in the next paragraph) it is known that the velocity in the

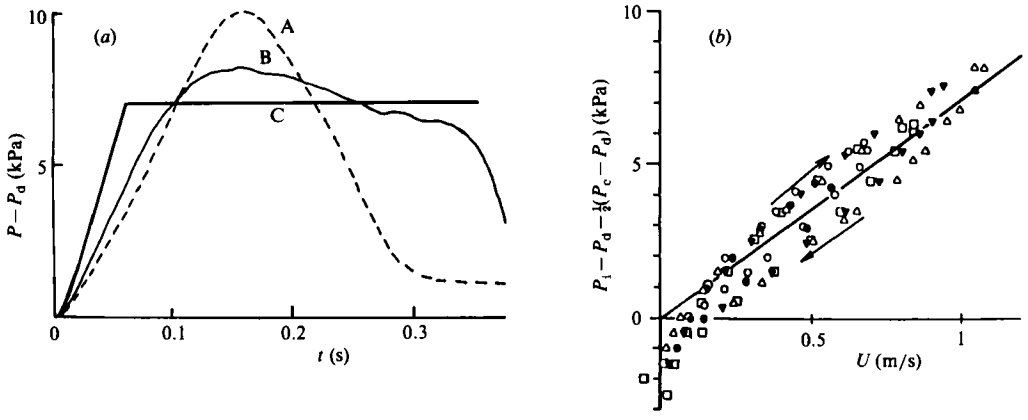

FIGURE 8. Comparison of experimental results and analytical results for idealized collapsible-tube model at $x = -2.5$ cm, $P_d = 4$ kPa. (*a*) Pressure waves at $P_d - P_c = -7$ kPa: A, incident pressure wave; B, measured pressure wave; C, result of idealized model tube. (*b*) Relations between the velocity wave U in the fully collapsed condition and the incident pressure wave P_i. ——, result of idealized model tube at $P_d - P_c = -7$ kPa; symbols, experimental results for various $P_d - P_c$ values (△, $P_d - P_c = -3$ kPa; ▼, -5 kPa; □, -7 kPa; ○, -9 kPa; ●, -11 kPa).

collapsed segment does not exceed 1.7 m/s, and the corresponding velocity in the inflated proximal tube is about 0.9 m/s. The pressure difference due to the flow acceleration at $x = 0$ is less than 1.04 kPa at maximum. Strictly speaking this is not small enough to ignore, but, for simplicity, it is neglected here and the pressure in the inflated tube proximal to the box is assumed to be $P_c - \Delta P$ when there is flow into the collapsed segment. This is equivalent to the tube proximal to the box having an open end at $x = 0$. From the one-dimensional-flow assumption and (1), the pressure P and the mean velocity U_m at the inlet of the box thus become

$$\left.\begin{aligned} P - P_d &= P_c - \Delta P - P_d, \\ U_m &= \frac{2}{\rho C}\{(P_i(t) - P_d) - \tfrac{1}{2}(P_c - \Delta P - P_d)\} \quad \text{for } P_i(t) - P_d > \tfrac{1}{2}(P_d - \Delta P - P_d). \end{aligned}\right\} \tag{3}$$

Examples of the pressure waveform and the P_i versus U_m relation expressed by (2) and (3) are shown in figure 8(*a*, *b*) respectively by thick solid lines. In this case $P_d - P_c = -7$ kPa, ΔP is set to zero and C is 13 m/s. The experimentally obtained P-waveform and $P_i - P_d$ versus U relation for $P_d - P_c = -7$ kPa (shown by □) are also indicated in the figure. The experimentally obtained U differs from U_m, because of the development of an unsteady boundary layer, but for the present experimental conditions it is found from simulation that the difference is less than 10 % during the compression. The difference increases during the expansion, but the trend of change of U and U_m is similar. It should be noted that the results from this simplified model qualitatively explain the unique features of these experimental results quite well. The measured pressure wave, however, changes gradually in CP, corresponding to a change in Q, and sharply decreases when P reaches about $P_c - 1.4$ kPa. This gradual deviation of measurement from calculation is assumed to be a result of difference of impedance between the idealized and the real tubes. The impedance of the idealized tube is zero when it begins to open, while that of the real one is small but non-zero. Therefore the measured value of P changes a little, corresponding to a Q-change. The sharp P drop in TP is explained as follows. Near the end of the CP, the fluid in the

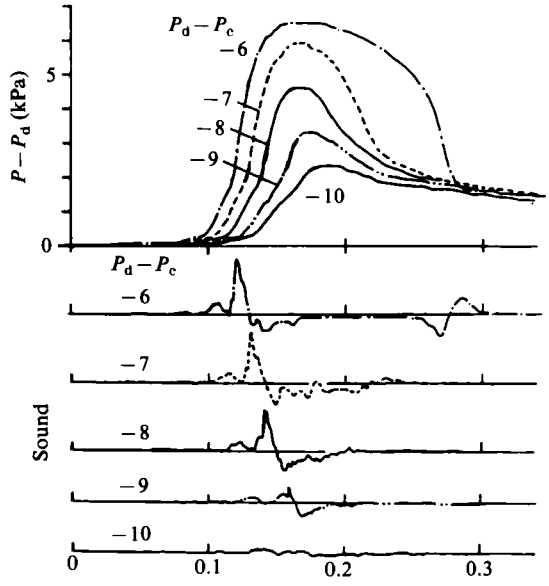

FIGURE 9. Pressure waves and sounds monitored at $x = 21.5$ cm for various $P_d - P_c$ values, $P_d = 4$ kPa.

partially collapsed segment in the box is considered to be pushed out into the inflated proximal segment by the high P_c, and hence the situation is similar to that in the experiment conducted by Kamm & Shapiro (1979). In such a situation, the flow tends to be choked near the proximal end of the partially collapsed segment in the box, and a severe local constriction, which decreases the flow rate sharply, is formed. In this experiment too, such a local constriction is formed at the start of the TP.

To check the validity of the simplified model further, experimental values of U over a wide range of P_c are also plotted in figure 8(*b*). The incident pressure wave $P_i(t)$ is the same for all the P_c cases. The plots for various P_c values agree well with each other. From (3) and the approximation $A(P) = A(P_d)$; the change due to P for inflated tubes is very small, and the flow rate Q penetrating into the fully collapsed tube segment may be expressed as

$$Q = U_m A = \frac{2}{\rho C}\{P_i(t) - P_d - \tfrac{1}{2}(P_c - P_d)\} A(P_d) \quad \text{for } P_i(t) - P_d - \tfrac{1}{2}(P_c - P_d) > 0, \quad (4)$$

where C is constant at 13 m/s. This equation illustrates the important fact that the flow rate penetrating into the collapsed segment decreases with increases in P_c or decreases in P_i, but the influence of P_i is twice that of P_c.

3.3.2. *The origin of Korotkoff sound*

As seen in figures 7 i(*b*) and ii(*b*), the change of the pressure waveform due to P_c variation at the exit of the pressure box is complicated. The pressure waves, however, always have a steep wave front if P_c is lower than some critical value. Initially we will treat only the steep wave front, leaving the rest of the wave for subsequent discussion.

The wave front consists of a small rather gentle first step and a steeper, larger second step. Synchronized with the second step, a sharp single sound is emitted. Some examples of sounds monitored by the microphone set on the inflated tube at $x = 21.5$ are shown in figure 9 along with the simultaneously measured pressure waves. The

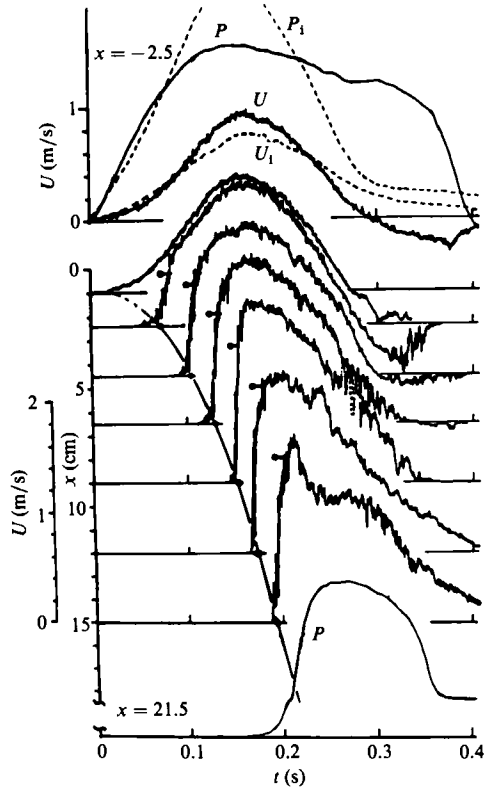

FIGURE 10. Pressure waveforms and velocity waveforms measured at various locations along the tube axis in and around the collapsed tube segment for $P_d - P_c = -6$ and 4 kPa, $P_d = 4$ kPa. Top, waveforms at $x = -2.5$ cm: P_i, incident pressure wave ($P_d = 0$); P, pressure wave for $P_d - P_c = -6$; U_i, incident velocity wave ($P_c = 0$); U, velocity wave for $P_d - P_c = -6$. Middle, velocity waves in the collapsed segment for $P_d - P_c = -6$. Bottom, pressure wave at $x = 21.5$ cm for $P_d - P_c = -6$ kPa. In the area where broken lines are used the change of the velocity waveform due to the perturbation was seen but it was difficult to determine its maximum.

amplitude of the steep second step of the pressure-wave front decreases with increases in P_c, and disappears if P_c becomes greater than some critical value. Corresponding to the pressure waveform change, the amplitude of the sound decreases, and finally the sharp sound disappears. Since this sound is assumed to be Korotkoff sound, the fluid-dynamical mechanism producing the steep second step at the wave front is the key to deciphering the origin of Korotkoff sound at high cuff pressures.

To find the fluid-dynamical mechanism, the fluid velocity in the collapsed tube segment is measured at various locations along the tube axis. One example of a set of velocity waveforms for $P_d - P_c = -6$ kPa is shown in figure 10. It is seen from the figure that the front of the velocity wave becomes steep very rapidly once it penetrates into the fully collapsed segment, and the amplitude of it increases with the distance of travel x. Synchronized with the arrival of the steep velocity-wave front at the distal end of the collapsed tube segment, the steep second step appears on the pressure waveform at $x = 21.5$. The propagation velocity of the velocity-wave front increases with x. The propagation velocities calculated from the gradient of the solid line shown in the figure, which connects smoothly the timings of the wave-front

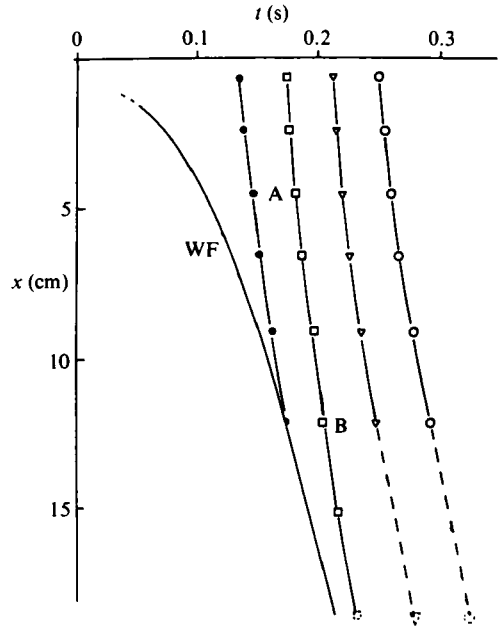

FIGURE 11. Propagation courses on (t, x)-plane of the wave front and marker waves put on various parts of incident pressure wave for $P_d - P_c = -6$ kPa, $P_d = 4$ kPa; WF, wave front.

appearance from each velocity measurement location, are shown by a short horizontal line with a black circle on each velocity diagram. It should be noted that the wave-front propagation velocity agrees well with the wave-front flow velocity.

Behind the wave front the tube is observed to be in a partially collapsed condition; therefore the part of the wave following the front is considered to propagate as a pressure wave with a velocity equal to the sum of the flow velocity U and the pressure-wave propagation velocity C_w determined from the tube law and corresponding transmural pressure). Thus the part following the wave front may travel faster than the wave front itself. This consideration leads us to conclude that the formation of the steep wave front is again caused by an overtaking phenomenon, as in the low-cuff-pressure condition.

To examine the validity of this hypothesis, a small single pressure wave is put on various parts of the incident wave, as a mark, by a single push of a plunger set on the rubber tube at $x = -30$ cm, and the travelling of the mark is followed by flow-velocity measurements at various x-values. The path of the maximum-amplitude portion of the marking wave on the (t, x)-plane is shown in figure 11 for $P_d - P_c = -6$ kPa. From the figure it is clearly seen that parts of the pressure wave behind the wave front propagate faster than the wave front, and thus certain portions catch up with the wave front.

Now, let us examine the flow condition in the fully collapsed tube. Every part of the wave except the wave front is assumed to be propagated at a velocity U_t, which is the summation of the flow velocity U and the propagation velocity C_w of small pressure wave:

$$U_t = U + C_w. \tag{5}$$

U_t is calculated from the gradient of the marking-wave travelling lines in figure 11,

and U is known from figure 10. In the region of collapsed tube segment near the inlet, for example at point A in figure 11,

$$U_t = 3.7 \text{ m/s}, \quad U = 1.3 \text{ m/s}, \quad C_w = 2.4 \text{ m/s}.$$

Since in this case $U < C_w$ the flow is subcritical. But, going downstream, U increases gradually and U_t decreases. For example, at point B

$$U_t = 2.9 \text{ m/s}, \quad U = 1.5 \text{ m/s}, \quad C_w = 1.4 \text{ m/s}.$$

In this case U and C_w are almost the same, and hence the flow is in the critical condition. Similar results are obtained for other P_c values, and hence it can be said that the flow condition corresponding to pressure-wave propagation in a fully collapsed tube segment becomes high subcritical or supercritical over the distal-half region of the collapsed segment.

3.3.3. *Phenomena occurring at the distal end of the collapsed tube segment*

The characteristics of pressure waveform variation at the box exit change at some critical P_c value, P_{ccrit}, which is $P_d + 6.5$ kPa in the present experimental condition (see figure 7i(*b*), ii(*b*)). As for the maximum amplitude, it increases gradually with increases in P_c for $P_c < P_{ccrit}$, but decreases rapidly for $P_c > P_{ccrit}$. With regard to the pressure waveform, if $P_c < P_{ccrit}$ it consists of a steep wave front (WF), a gradually decreasing central part (GD), and a rapidly decreasing tail part (RD). The transition from GD to RD occurs at $P = P_c - 1.4$ kPa for all P_c values, as seen in the pressure waves at the box inlet. However, if $P_c > P_{ccrit}$, the GD part disappears and the pressure wave becomes similar to a single-peak wave.

As mentioned in §3.3.1, the amplitude of the flow rate penetrating into the fully collapsed tube segment in the box decreases monotonically with increasing P_c. Furthermore, the amplitudes of velocity waves measured at the same x in the fully collapsed segment are observed to decrease systematically with increases in P_c. Therefore the question arises as to the origin of the complicated change of the pressure waveform at $x = 21.5$. It is thought to be a phenomenon of the box exit, where the fully collapsed and the inflated tube segments are connected.

In order to understand the phenomena at the distal end of the collapsed segment, the fluid velocity near there and the change of the longitudinal tube shape will be examined. In this experiment the type 2 tube is used because of the opacity of the cast silicone rubber used in the type 3 tube. As was shown in figure 5, the main parts of the pressure waves in both types 2 and 3 tubes at $x = 21.5$ are almost the same, and hence similar phenomena will occur at the collapsed distal end of both tubes.

As seen in figure 7i(*a*), when P_c is low, a portion of the steep wave front (shock wave) arriving at the distal end is reflected and propagates upstream as a shock wave. An example of a series of measured tube longitudinal shapes for $P_d - P_c = -3$ kPa is shown in figure 12(*a*). H values are measured from still photographs taken at the various instances indicated in figure 12(*b*). This figure also shows the pressure measured at $x = 21.5$ and the tube central velocity at $x = 18$. As indicated by line 0 in figure 12(*a*), the tube distal and proximal end regions, over a length of about 1.5 cm, do not collapse completely, because of an end effect. The opening of the most distal part of the fully collapsed region ($x = 17$) (line 5), coincides with the appearance of the steep second step of the pressure-wave front at $x = 21.5$ and of the steep velocity-wave front at $x = 18$. In a very short period following the opening of the distal end (i.e. the beginning of reflection) a couple of small humps with short wavelength appear over the proximal region and propagate upstream at almost the

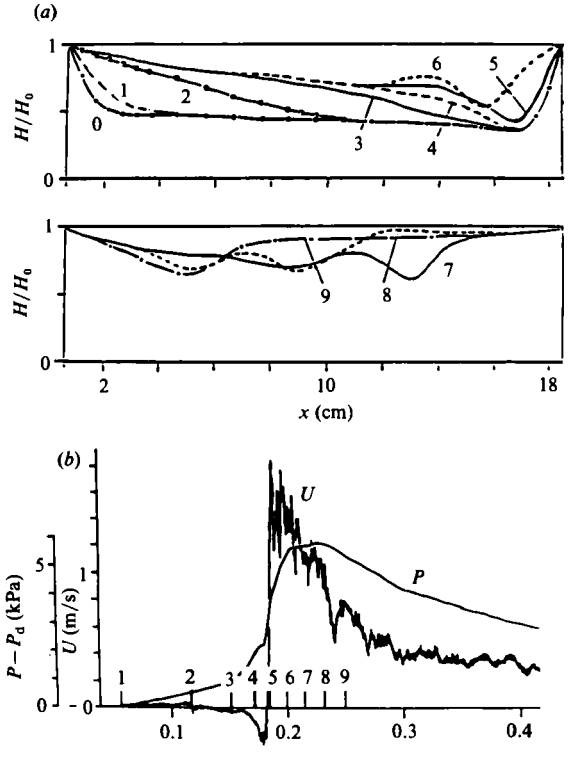

FIGURE 12. Longitudinal tube shapes and velocity at the box exit for $P_d - P_c = -3$ kPa, $P_d = 4$ kPa. (*a*) Variation of longitudinal shape of fully collapsed tube segment at various instances indicated in (*b*): H, tube height; H_0, tube height at $P_c = 0$. (*b*) Velocity U at $x = 18$ and pressure P at $x = 21.5$ cm.

same speed as the reflected shock wave. These small waves preceding the shock are considered to be similar to those observed by Kececioglu *et al.* (1981) in steady flow transition from supercritical to subcritical flow, and hence are thought to be caused by the axial tension of the tube.

Corresponding to P_c augmentation, the positive reflection at the distal end of the collapsed segment weakens and the propagation velocity of the reflected wave greatly decreases. The maximum P_c value for which positive reflection is seen is found to be P_{ccrit}. The tube-shape diagram for $P_d - P_c = -6$ kPa is shown in figure 13(*a*), and the fluid velocity at the tube centre at $x = 18$ and the pressure at $x = 21.5$ are also shown in figure 13(*b*). Again, coinciding with the arrival of the steep wave front, the distal end of the collapsed tube segment begins to open and, at the same time, a hump appears over a short proximal region (lines 3 and 4 in figure 13*a*). However, the reflected wave and the hump do not propagate upstream so much. As seen in the figure 13(*b*), the central velocity at $x = 18$ is negative until the arrival of the steep second step of the wave front and also after the RD portion of the pressure wave, but is maintained at a relatively high positive constant value during the intermediate period. At $x = 18$ the tube is deformed in a complicated manner because of the end effect, and the central part always opens slightly. Therefore the reverse flow at the tube centre indicates that a tube portion just proximal to $x = 18$ collapses fully to make a severe constriction, and that the fluid coming out through the two thin channels left open on the sides makes a pair of jets. The high positive velocity between the wave front and RD indicates the slight opening of the constricted portion.

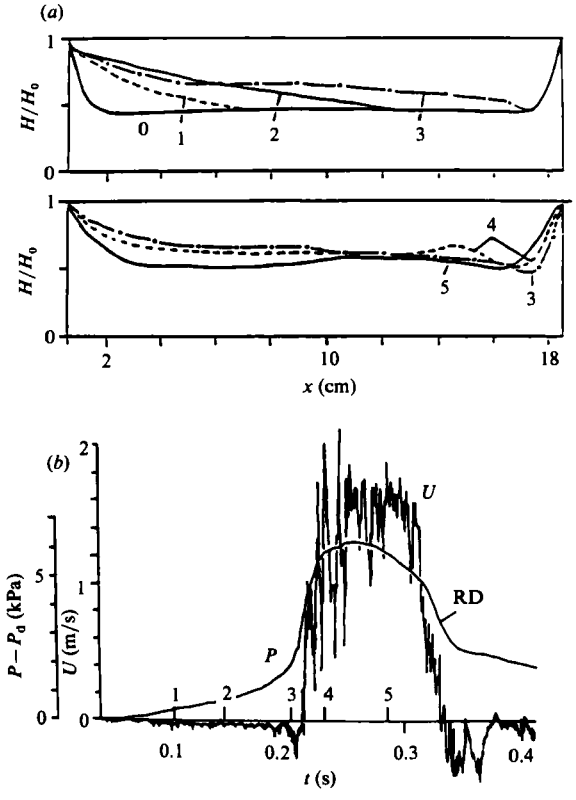

FIGURE 13. Longitudinal tube shapes and velocity at the box exit for $P_d - P_c = -6$ kPa, $P_d = 4$ kPa. (*a*) Variation of longitudinal shape of fully collapsed tube segment at various instances indicated in (*b*): H, tube height; H_0, tube height at $P_c = 0$. (*b*) Velocity U at $x = 18$ and pressure P at $x = 21.5$ cm.

When P_c is raised above P_{ccrit}, the tube height H increases a little over the region $x < 17.5$, but no tube shape change is seen over the region of $x > 17.5$, and hence it is expected that the central portion of the collapsed tube near the distal end is kept closed throughout this period. Fluid-velocity measurements support this expectation. The velocities at $x = 18$, measured at the tube centre and at a location near the side tube, are shown in figure 14 for $P_d - P_c - 7$ kPa, in which the pressure waveform at $x = 21.5$ is also shown by a broken line for reference. At the tube centre the fluid velocity is very low even in the period corresponding to the main part of the pressure wave, while, on the side, a very high velocity of about 3 m/s is seen. Thus it has been found that, for $P_c > P_{ccrit}$, no wave reflection occurs at the box exit, there always exists a short fully collapsed tube portion (the constriction) near the end of the tube in the box, and the flow becomes two high-speed jets behind the constriction.

The abovementioned phenomenon at the box exit suggests that the form of the pressure wave at the box exit depends on whether positive reflection occurs at the box exit or not. In order to examine the validity of this hypothesis and to discover what determines P_{ccrit}, the experiments described below are planned based on the following consideration.

As mentioned above, the tube in the box is forced into a partially collapsed condition by the propagated pressure wave, and hence the static pressure of the pressure wave is nearly equal to P_c. The factors that determine the reflection

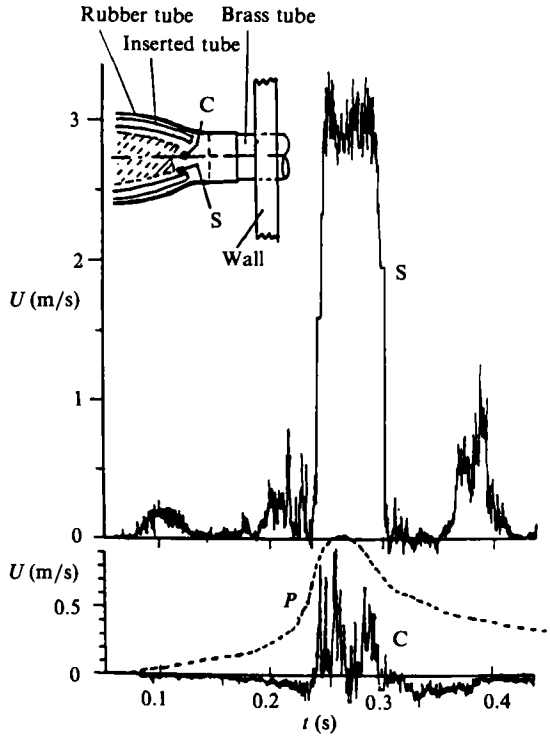

FIGURE 14. Velocities at the tube centre and near the side tube at $x = 18$ cm; C, central velocity; S, velocity near a side tube; P (– – – –), pressure at $x = 21.5$ cm. Schematic diagram on the top shows measurement locations for C and S.

condition at the box exit are the energy and the flow rate of the pressure wave travelling through the fully collapsed tube segment and the initial pressure of the tube distal to the box (P_{dd}). In the experiments discussed so far P_c is changed, and therefore both the energy and the flow rate of the pressure wave reaching the box exit are changed. The type 3 tube, however, has almost zero cross-sectional area in the fully collapsed condition, and hence P_{dd} can be altered arbitrarily without affecting conditions in and proximal to the box. Thus, for the same pressure wave, the reflection condition at the box exit can be altered by changing P_{dd}.

The following experiments parallel those previously described. However, the initial pressure P_d of the proximal tube and the box pressure P_c are kept constant and the initial pressure of the distal tube P_{dd} is changed. An example of a set of pressure waves at the inlet and exit of the box for various P_{dd} values are shown in figure 15(a, b) respectively. In this case the transmural pressure in the box based on P_d is -7 kPa ($P_d - P_c = -7$). Therefore $P_c > P_{ccrit}$ when $P_{dd} = P_d$. P_{dd} is changed from $P_d - 2$ to $P_d + 5$. The pressure wave at the box inlet (figure 15a) is not affected by this P_{dd} change except for the appearance of small waves, considered to be reflected shock RSW, in the highest-P_{dd} case. Furthermore, the timing of the steep wave front's appearance at the box exit coincides for all P_{dd} cases. Therefore the pressure-wave propagation in the collapsed tube segment is considered to be same for all the cases.

At the box exit the pressure waveform does not change much when P_{dd} is decreased from P_d. However, it changes greatly when P_{dd} is increased above P_d and the gradually decreasing wave portion (G) followed by a rapid descending region (R) appear (as in the $P_c < P_{ccrit}$ condition). Corresponding to this waveform change, the

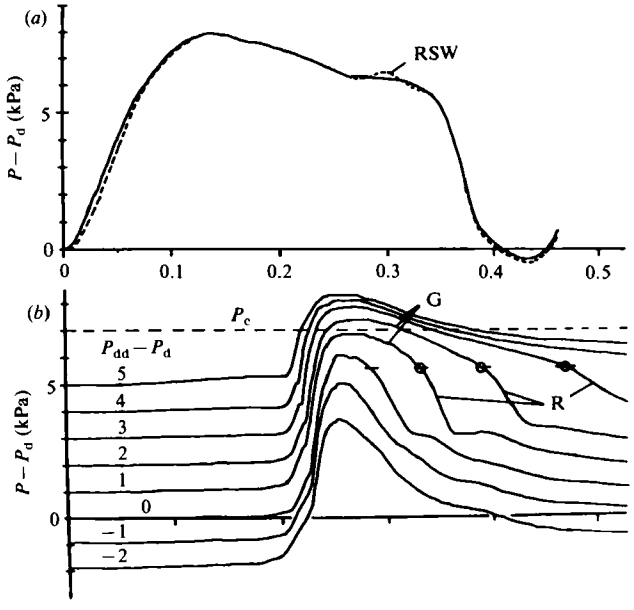

FIGURE 15. Variation of pressure waveform due to change in distal initial tube pressure P_{dd} for constant $P_d - P_c = -7$, $P_d = 4$ kPa; (*a*) pressure waveform at $x = -2.5$ cm; RSW, reflected shock wave, (*b*) pressure waveforms at $x = 21.5$ cm; G, gradually descending portion; R, rapid-descending portion.

maximum amplitude of the pressure wave $P_{max} - P_{dd}$, appearing just behind the wave front, is found to decrease with increases in P_{dd}.

Let us consider the change in P_{max} first. From (1) and the assumption that the cross-sectional-area change of the inflated tube due to pressure variation is negligibly small; $A(P) = A(P_{dd}) \equiv A_0$, the flow rate Q in the inflated tube distal to the box is then expressed as

$$Q = \frac{A_0}{\rho C_0}(P - P_{dd}), \tag{6}$$

where C_0 is the wave-propagation velocity at $P = P_{dd}$. Thus

$$Q_{max} = \frac{A_0}{\rho C_0}(P_{max} - P_{dd}). \tag{7}$$

Therefore reduction of $P_{max} - P_{dd}$ means reduction of Q_{max}. It is not known exactly whether this means an increase in the positive reflection or a decrease in the negative reflection, but the former is thought more likely because of the relationship between P_{max} and P_c. The change of the pressure waveform at the box exit is similar for other P_c cases.

In order to understand what happens when positive reflection at the box exit does not occur, Q_{max} variation due to changes in P_{dd} are now examined. Q_{max}, calculated from (7) and the measured P_{max} at $x = 21.5$, is shown in figure 16 for various $P_d - P_c$ cases. The inclined solid lines indicate (7) for various P_{dd}. For all P_c values, when P_{dd} is higher than some critical value, Q_{max} increases with decreasing P_{dd}, but, when P_{dd} is below the critical value, Q_{max} becomes almost constant and then decreases slightly with further decreases in P_{dd}. This transition occurs always when P_{max} becomes nearly equal to P_c.

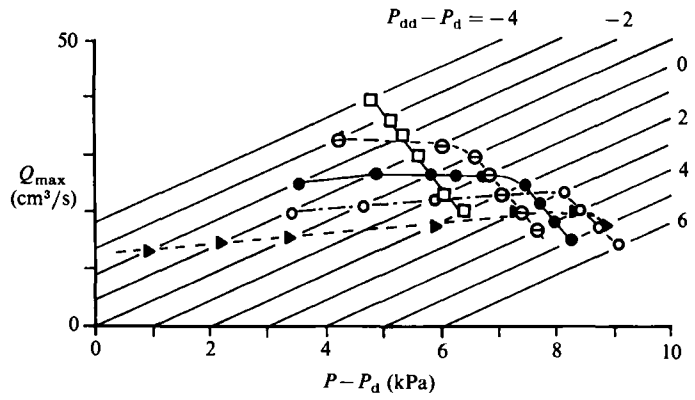

FIGURE 16. Variation of maximum flow rate Q_{max} at $x = 21.5$ cm due to P_{dd} change for various $P_d - P_c$ values; □, $P_d - P_c = -4$ kPa; ⊖, −6 kPa; ●, −7 kPa; ○, −8 kPa; ▶, −9 kPa; inclined solid lines, equation (7) for various $P_{dd} - P_d$ values.

From these experimental results, the phenomenon occurring at the box exit may be described as follows. When the maximum flow rate of the pressure wave arriving at the distal end of the collapsed segment, Q_{maxc}, is high and the corresponding P_{maxc} calculated from (7) exceeds P_c, positive reflection occurs at the box exit, and the fully collapsed tube portion near its distal end opens up to the centre. However, when P_{dd} (or Q_{maxc}) decreases and P_{maxc} becomes nearly equal to or lower than P_c, no wave reflection occurs at the box exit, and a short tube segment just proximal to the box exit is kept in a fully collapsed condition. Thus the flow becomes high-speed jets which produce large energy loss. Since, in no reflection case, the maximum flow rate is maintained almost constant despite P_{dd} change, the energy loss at the box exit should increase in proportion to $P_c - P_{dd}$. Therefore the constriction has to become more severe with increasing $P_c - P_{dd}$ to augment the jet speed and the friction loss at the constriction.

P_{ccrit}, at which the positive reflection at the box exit ceases to occur, is known to depend on both Q_{maxc} and P_{dd}. Q_{maxc} depends on the amplitude of the incident pressure wave and possibly on the form of the incident wave and the length of the collapsed segment, as predicted from the velocity waveform diagram in figure 10. Therefore P_{ccrit} depends on all these factors.

Let us consider the waveform change next. As mentioned before, G- and R-portions appear when positive wave reflection occurs at high P_{dd}, and the G–R transition occurs at the same P-value of $P_c - 1.4$ kPa as in the pressure wave at the box inlet. In the present experiment the pressure waves in the collapsed segment are identical for all P_{dd} cases, but the duration of G changes greatly with P_{dd}. This fact indicates that the flow in the G-portion is not affected by the form of the pressure wave travelling through the collapsed segment. Hence it appears that, over the G-portion, the flow situation is similar to that in the box inlet, and the fluid in the collapsed segment is pushed out into the distal inflated tube by P_c. For all $P_c > P_{ccrit}$, the hump in the tube longitudinal shape, as seen on line 4 in figure 13, is observed in the region just proximal to the constriction, and it takes a relatively long time for the tube shape to return to the initial shape.

The experimental results mentioned above show that P_{dd} becomes another independent variable governing pressure-wave propagation if the tube segment in the box collapses completely. Therefore it is necessary to keep $P_{dd} - P_c$ constant to know

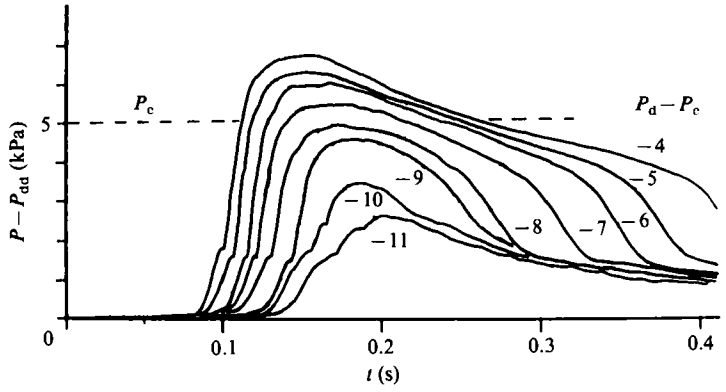

FIGURE 17. Comparison of pressure waveforms at $x = 21.5$ for various $P_d - P_c$ cases for constant $P_{dd} - P_c$ condition, $P_{dd} - P_c = -5$ kPa; $P_d = 4$ kPa.

the effect of P_c variation on the pressure wave arriving at the distal end of the fully collapsed segment. Pressure waves at $x = 21.5$ with $P_{dd} - P_c = -5$ kPa are shown in figure 17 for various $P_d - P_c$ cases. The amplitude of the pressure wave decreases systematically with increasing P_c, which corresponds well with the systematic changes of flow rate at the box inlet.

3.3.4. *Effect of incident pressure-wave amplitude*

According to the experimental results obtained in §3.3.1, the flow rate penetrating into the fully collapsed tube segment in the box is determined by (4) as

$$Q(t) = \frac{2}{\rho C}\{P_i(t) - P_d - \tfrac{1}{2}(P_c - P_d)\}A(P_d) \quad \text{for } P_i(t) - P_d - \tfrac{1}{2}(P_c - P_d) > 0. \tag{4}$$

Therefore, in certain cases, the same $Q(t)$ can be obtained for different $P_i(t)$ by changing P_c. The transmural pressures $P_c - P_d$, however, are different in each P_i case, and hence the pressure waves arriving at the distal end of the collapsed tube may be different. However, when the law of the type 3 tube is considered, the pressure P at which the tube begins to open is $P_c - \Delta P$, and the pressure proximal to the box goes up to that level by positive reflection before the beginning of wave penetration, and hence the effective transmural pressure in the box should be considered as $-\Delta P$ (constant value). If this is true, it can be said that pressure-wave propagation in the fully collapsed tube segment depends only on $Q(t)$ and that pressure waves arriving at the distal end of the collapsed segment become identical, regardless of the values of $P_i(t)$ and P_c, for all cases in which $Q(t)$ is the same. In order to verify this hypothesis, a series of experiments with different-amplitude incident waves are conducted.

Three incident pressure waves $P_{i1}(t)$, $P_{i2}(t)$ and $P_{i3}(t)$ and the corresponding velocity waves to be used in this experiment are shown in figure 18. The conditions for each incident-wave case are expressed by subscript n ($n = 1, 2, 3$). In order to make the incident waves satisfy the following equation (8), the stroke and the rotation speed of the pump were adjusted:

$$P_{in}(t) = \begin{cases} P_{i1}(t) - D_n & \text{for } P_{i1}(t) - D_n > 0, \\ P_d & \text{for } P_{i1}(t) - D_n < 0, \end{cases} \tag{8}$$

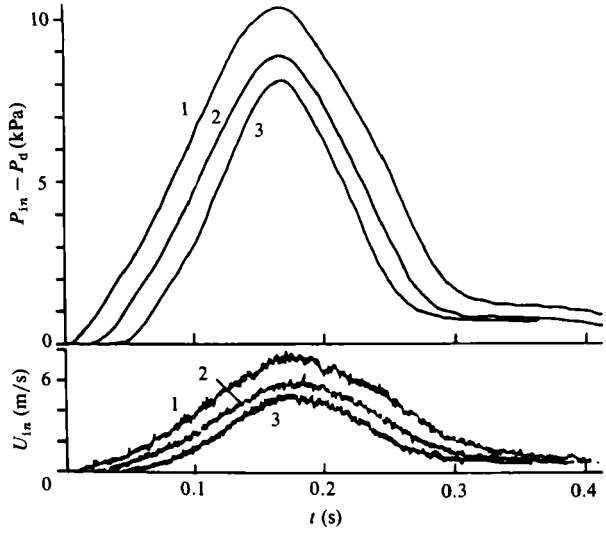

FIGURE 18. Pressure and velocity waveforms at $x = -2.5$ cm for three different incident pressure waves, $P_D = 4$ kPa; 1, 2 and 3 are for the incident pressures of P_{11}, P_{12} and P_{13} respectively.

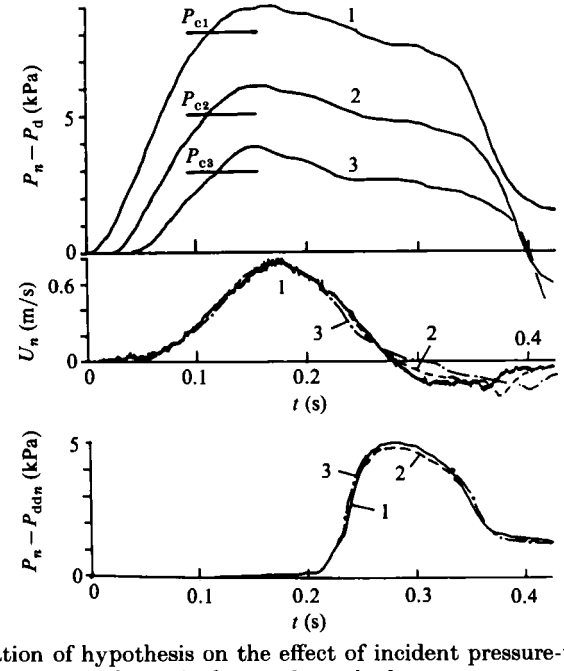

FIGURE 19. Verification of hypothesis on the effect of incident pressure-wave amplitude; results for the three incident waves, shown in figure 18, at the box pressures satisfying (9); $P_d = 4$ kPa, 1, $P_d - P_{c1} = -8$; 2, $P_d - P_{c2} = -5$; 3, $P_d - P_{c3} = -3$ kPa; top, pressure waves at $x = -2.5$ cm; middle, velocity waves at $x = -2.5$ cm; bottom pressure waves at $x = 21.5$ cm.

where D_n is the difference of the amplitude between the 1st and the nth incident pressure waves. As seen in the figure, however, (8) is not completely satisfied. Therefore the D_n are taken as time-mean values, and they are $D_2 = 1.5$, $D_3 = 2.5$ kPa. The P_{cn} producing the same $Q(t)$ wave are obtained from (4) and (8) as

$$P_{cn} = P_{c1} - 2D_n. \tag{9}$$

As concluded in §3.3.3, the pressure difference $P_{dd}-P_c$ at the box exit has to be the same for the pressure waveform arriving at the box exit to be known. Thus

$$P_{ddn} = P_{dd1} - 2D_n. \tag{10}$$

Many experiments have been conducted for various P_{c1} and P_{dd} values. An example of the experimental results is shown in figure 19. In this case, $P_d-P_{c1}=-8$, $P_d-P_{c2}=-5$ and $P_d-P_{c3}=-3$ kPa and $P_{ddn}-P_{cn}=-5$ kPa. The top graph is the pressure wave at $x=-2.5$, the middle graph is the velocity at the same location, and the bottom graph is the pressure at $x=21.5$. As seen in the middle figure, the condition that $Q(t)$ be the same in all cases is satisfied fairly well. From the bottom figure, all the pressure waves are seen to be almost identical. Under other experimental conditions, the same results are also obtained, and the hypothesis mentioned above is thus verified.

4. Conclusion

From the experimental study mentioned above, the following knowledge has been gained of the propagation characteristics of single half-sinusoidal pressure waves in a fully collapsed tube segment with long distended tube segments on both proximal and distal sides.

1. For a tube having zero cross-sectional area in the fully collapsed condition, the flow rate Q of the pressure wave penetrating into the fully collapsed tube segment is expressed approximately by the following equations:

$$Q = 0 \quad \text{for } P_i(t)-P_d) < \tfrac{1}{2}(P_c-P_d),$$

$$Q(t) = \frac{A(P_d)}{\rho C}\{P_i(t)-P_d-\tfrac{1}{2}(P_c-P_d)\} \quad \text{for } P_i(t)-P_d > \tfrac{1}{2}(P_c-P_d).$$

Therefore Q decreases with both increasing P_c and decreasing $P_i(t)$, but the effect of $P_i(t)$ on Q is twice as strong as that of P_c.

2. The characteristics of pressure-wave propagation in a fully collapsed tube segment are identical regardless of the value of the virtual transmural pressure P_d-P_c. This is because the effective transmural pressure is the difference between P_c and $P_c-\Delta P$, at which pressure the fully collapsed tube starts to open. Therefore the pressure wave that arrives at the distal end of the collapsed segment depends only on $Q(t)$, if the length of the collapsed segment is the same.

3. In a fully collapsed tube segment the propagation velocity of the wave front is approximately equal to the fluid velocity at the wave front, while the propagation velocity of the parts behind the wave front is the sum of the fluid velocity and the wave-propagation velocity for infinitely small waves, which is of the same order of magnitude as (and possibly greater than) the fluid velocity. Therefore the wave front is overtaken by other portions of the wave in the course of propagation, and becomes a very steep one (shock wave). This steep wave front produces a sharp thud sound when it propagates into the inflated tube segment distal to the box.

4. The flow condition in the collapsed segment is high subcritical or supercritical near the distal end. The amplitude and the form of the pressure wave penetrating into the inflated tube distal to the box depend on the maximum flow rate Q_{maxc} of the pressure wave arriving at the distal end of the collapsed segment, and the difference of the box pressure P_c and the initial pressure P_{dd} in the distal tube. When Q_{maxc} is large and P_{maxc} $(=P_{dd}+\rho C_0 Q_{maxc}/A_0)$ is higher than P_c, positive wave

reflection occurs at the box exit, and the distal end of the fully collapsed segment opens. In this case, the amplitude of the pressure wave in the distal inflated tube decreases with increasing $P_{dd}-P_e$, and the pressure waveform consists of a steep wave front, which produces Korotkoff sound, a central portion of gradual pressure decrement, and a tail portion of more rapid pressure decrement (in which the tube again closes at the distal end).

When P_{dd} or Q_{maxc} is low and P_{maxc} is smaller than P_e, no wave reflection occurs at the box exit, a strong constriction is made near the distal end of the collapsed segment, and the flow becomes two high-speed jets. In this case, Q_{maxc} is conserved, and hence the amplitude of the pressure wave in the distal inflated tube changes little with $P_{dd}-P_e$ variation. The form of the pressure wave becomes a single-peak shape, and has no gradual pressure-decrement portion. The wave front is still steep enough to produce sound when the flow rate is relatively large. The wave-front steepness, however, is reduced with flow-rate reduction.

REFERENCES

Burch, G. E. & De Pascuale, N. P. 1962 *Primer of Clinical Measurement of Blood Pressure.* C. V. Mosby.

Jan, D. L., Kamm, R. D. & Shapiro, A. H. 1983 Filling of partially collapsed compliant tubes. *Trans ASME* K: *J. Biomed, Engng* **105**, 12.

Kamm, R. D. & Shapiro, A. H. 1979 Unsteady flow in a collapsible tube subjected to external pressure or body forces. *J. Fluid Mech.* **95**, 1.

Kececioglu, I., McClurken, M. E., Kamm, P. D. & Shapiro, A. H. 1981 Steady, supercritical flow in collapsible tubes. Part 1, Experimental observations. *J. Fluid Mech.* **109**, 367.

Kenner, T. 1976 Pulse wave reflection at the collapsed segment of an artery in Riva-Rocci's method. *Pflügers Archiv* **364**, 285.

Lighthill, M. J. 1972 Physiological fluid dynamics: a survey. *J. Fluid Mech.* **52**, 475.

London, S. B. & London, R. E. 1964 Comparison of indirect pressure measurement (Korotkoff) with simultaneous direct brachial artery pressure distal to the cuff. *Adv. Intl Med.* **13**, 127.

London, S. B. & London, R. E. 1967 Critique of indirect diastolic end point. *Arch. Intl Med.* **119**, 39.

McCutcheon, E. P. & Rushmer, R. F. 1967 Korotkoff sounds. *Circulat. Res.* **20**, 149.

Pedley, T. J. 1980 *The Fluid Mechanics of Large Blood Vessels.* Cambridge University Press.

Shimizu, M. & Tanida, Y. 1983 On the mechanism of Korotkoff sound generation at diastole. *J. Fluid Mech.* **127**, 315.

Ur, A. & Gordon, M. 1970 Origin of Korotkoff sounds. *Am. J. Physiol.* **218**, 524.

Wallace, J. D., Lewis, D. H. & Khlil, S. A. 1961 Korotkoff sounds in humans. *J. Acoust. Soc. Am.* **33**. 1178.